

# Influence of water up-take on interlaminar fracture properties of carbon fibre-reinforced polymer composites

R. SELZER, K. FRIEDRICH

*Institute for Composite Materials Ltd, University of Kaiserslautern, 67663 Kaiserslautern, FRG*

Composite materials in practical use can be subjected to a wide variety of different loading conditions. The most important conditions are mechanical stresses and environmental attacks. An issue of major concern in the utilization of composites is associated with the occurrence of delaminations or interlaminar cracks, which may be related to manufacturing defects or are induced in service by low-velocity impacts. The main environmental attacks are temperature, humidity, radiation, and chemical exposure. Three materials were investigated; two thermosetting matrices (unmodified and toughness-modified epoxy, EP and EP<sub>mod</sub>) and one thermoplastic matrix (semicrystalline polyetheretherketone, PEEK), all reinforced with unidirectional continuous carbon fibres. Samples of these materials were exposed to water in baths of different temperatures; they were taken for mechanical testing after various time periods. As a result of absorbed moisture,  $G_{IC}$ -values increased with moisture content of the samples, whereas  $G_{IIC}$ -values decreased. By means of scanning electron microscopy, fracture surfaces were examined. Evidence was found that the increase of  $G_{IC}$ -values was due to a greater ductility of the matrix (as a result of the moisture absorbed) and hence more energy-consuming fibre-bridging. On the other hand, interface failure, as well as a loss of shear strength of the epoxy with increasing amount of moisture absorbed, were responsible for the decrease in the  $G_{IIC}$ -values. The thermoplastic matrix system (CF/PEEK) exhibited no influence of moisture on the Mode I property, but a decrease of the values for Mode II.

## 1. Introduction

Component parts made out of high-performance composite materials are subjected, like every other construction material in practical use, to mechanical stresses and to attacks from other environmental factors. Besides the possible influence of temperature, radiation and chemical attacks, the effect of moisture must always be taken into account. For example, moisture can be absorbed from the humidity in the atmosphere. The moisture affects the thermal and mechanical properties of the composites and therefore this fact cannot be neglected [1–3].

A very important topic in the use of composites is the occurrence of delaminations or interlaminar cracks, which may be related to manufacturing defects or are induced in service by low-velocity impacts. These delaminations can grow under different crack-opening modes [4]. To utilize the full potential of composite materials, their fracture mechanical behaviour under various environmental conditions must be determined. The goal of this work is to investigate the influence of moisture on the interlaminar fracture energies  $G_{IC}$  and  $G_{IIC}$  of carbon fibre-reinforced polymers.

## 2. Experimental procedure

### 2.1. Materials

The materials investigated were polymer matrices reinforced with unidirectional, continuous carbon fibres (CF). The first matrix, denoted here by EP, is a first generation epoxy, with a brittle fracture behaviour. It is characterized by a high Young's modulus, but a low fracture toughness. The second matrix, EP<sub>mod</sub>, is a new-generation resin with a higher strain to failure and a higher fracture toughness. For comparison, tests were done with carbon fibre-reinforced polyetheretherketone (PEEK). All specimens were made out of 16 plies with a foil in the middle, which is intended to have the same effect as a delamination. The carbon fibre volume fraction was  $60\% \pm 1\%$  for all materials studied.

### 2.2. Conditioning

First, the specimens were dried in an oven at  $77^\circ\text{C}$  until the specimen-weight was constant. Then the samples were exposed to water in baths of three different temperatures: 23, 70 and  $100^\circ\text{C}$ . Immersing samples in water is the worst possible moisture attack.

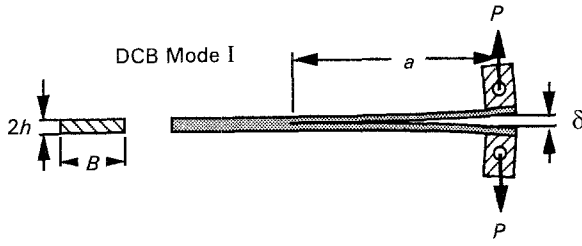


Figure 1 Mode I loading configuration.

Resting the specimen in humid air gives a lower maximum moisture content [5, 6]. After different periods of time, the specimens were taken out of the baths and subjected to the mechanical tests.

### 2.3. Mode I test

For Mode I tests, the double cantilever beam test configuration was used. The tests were performed according to a protocol of the European Group of Fracture [7]. The specimen considered was parallel-sided with a width of 20 mm. In the Mode I test, the tensile force is applied perpendicular to the direction of the fibres. The loading was introduced via machined loading blocks, which were bonded to the specimen (Fig. 1).

The loading of the sample took place in a Zwick universal testing machine at a constant rate of  $1 \text{ mm min}^{-1}$ . During the testing procedure, the crack length was measured visually at the specimen's edge

$$\text{moisture content} = \frac{\text{weight of specimen} - \text{weight of dry specimen}}{\text{weight of dry specimen}} \times 100 (\%) \quad (3)$$

using a travelling microscope. A thin layer of white ink facilitated this measurement. A plotter connected to the testing machine recorded the diagram of force versus crack opening displacement. The crack propagation was marked into the diagram. To calculate the critical energy release rate,  $G_{IC}$ , the corrected beam theory was used

$$G_{IC} = \frac{3Pd}{2(a + \Delta)B} \quad (1)$$

where  $P$  is the force,  $d$  the displacement,  $a$  the crack length and  $B$  the specimen width. The corrected beam theory requires the determination of a correction factor,  $\Delta$ , to the crack length for taking into account crack-tip rotation and shear deformation. This correction was obtained by plotting compliance to the one-third power,  $C^{1/3}$ , against crack length,  $a$ .  $\Delta$  was the intercept on the  $x$ -axis [8].

### 2.4. Mode II test

For the Mode II tests, an end-notched flexure (ENF) specimen geometry was used. In the Mode II test, crack propagation is induced by shear stresses. Owing to the bending, shear stresses develop along the neutral plane of the specimen. The specimen was loaded in a standard three-point bending fixture at a crosshead speed of  $0.5 \text{ mm min}^{-1}$ . In order to allow direct com-

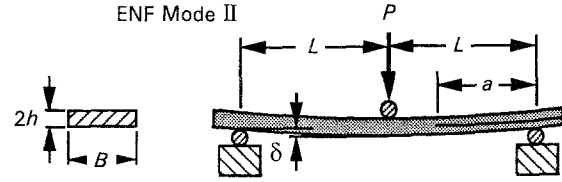


Figure 2 Mode II loading configuration.

parison of results, the distance between supports,  $2L$ , was fixed at 100 mm. The ratio of crack length to half span,  $a/L$ , was chosen to equal 0.5 (Fig. 2).

A plotter connected to the testing machine recorded the force versus bending displacement. The values of  $G_{IIC}$  are calculated from the direct beam theory by using the following expression

$$G_{IIC} = \frac{9a^2Pd}{2B(2L^3 + 3a^3)} \quad (2)$$

The parameters of this equation are the same as for Equation 1.

## 3. Results and discussion

### 3.1. Moisture absorption

The specimens were placed in water at three different temperatures. After various periods of time the specimens were taken out of the bath. The weight was measured with an analytical balance and the weight gain was calculated according to the equation

Figs 3–5 show the moisture absorption curves of the three materials used.

The results presented in the preceding graphs were averaged from measurements of 3–6 specimens prepared under identical conditions. As can be seen in all diagrams, the moisture absorption tends towards an equilibrium value, which depends on the material. The maximum moisture content of CF/EP, CF/EP<sub>mod</sub> and CF/PEEK were 1.6, 2.5 and 0.3 wt %, respectively. The higher the water temperature, the faster the specimens absorbed moisture and the faster the curves reached the saturation level.

### 3.2. Mode I fracture behaviour

The specimens were tested under three conditions: dry, half saturated and fully saturated. Tests were performed at room temperature in a laboratory air environment. During the testing procedure, a clear difference between the dry and wet specimens was observed.

Fig. 6 shows a typical dry specimen in a Mode I test. The region behind the crack opening over which the fibres are bridging is not very large. The fibres break almost immediately after the crack opening. Fig. 7 shows a photograph of a specimen which is completely saturated. Here the fibres are bridging over a large zone and are under stress.

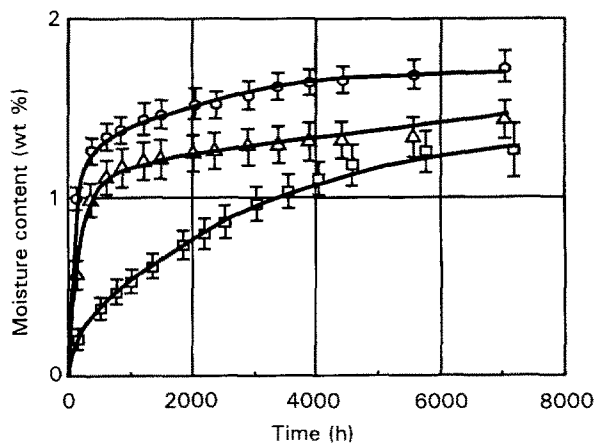


Figure 3 Moisture absorption curve of CF/EP, at (□) 23°C, (Δ) 70°C and (○) 100°C.

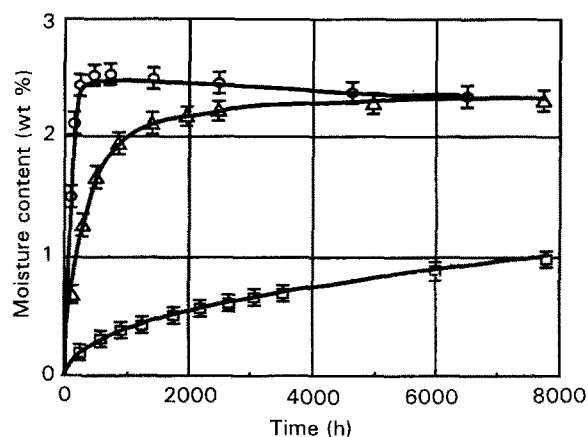


Figure 4 Moisture absorption curve of CF/EP<sub>mod</sub>, at (□) 23°C, (Δ) 70°C and (○) 100°C.

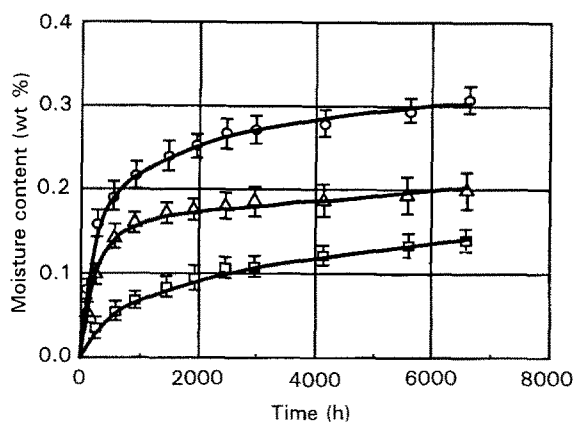


Figure 5 Moisture absorption curve of CF/PEEK, at (□) 23°C, (Δ) 70°C and (○) 100°C.

The variation of the  $G_{IC}$  values of CF/epoxy as a function of moisture content and temperature is shown in Fig. 8.

Mode I values of CF/EP<sub>mod</sub> are much higher than those of CF/EP. However, the toughness of CF/EP increases with increasing moisture content more than in the case of the modified epoxy. The curves of the  $G_{IC}$  values of the CF/EP<sub>mod</sub> specimens plotted against the moisture content exhibit an unusual behaviour. It

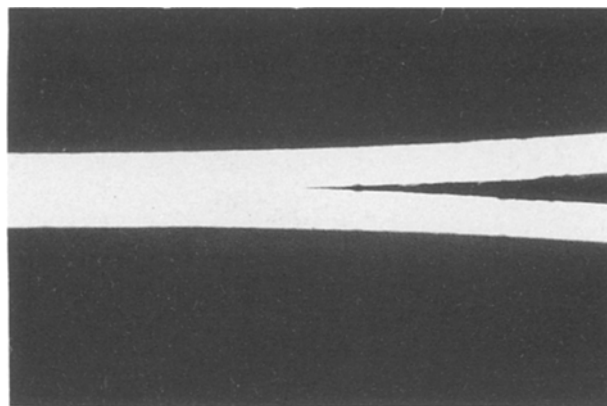


Figure 6 Fibre-bridging in a dry specimen.

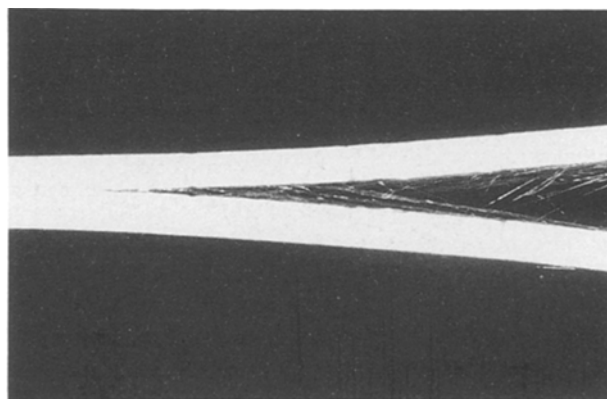


Figure 7 Fibre-bridging in a wet specimen.

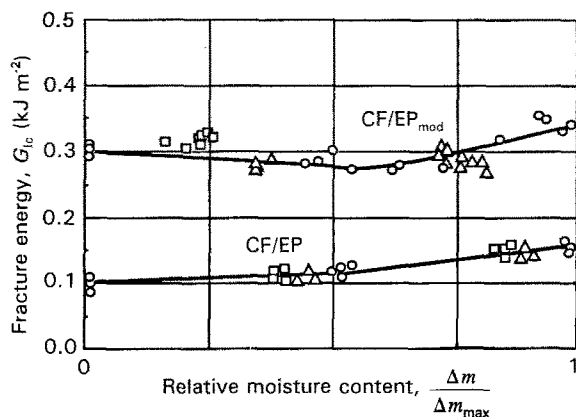


Figure 8 Results of the Mode I tests versus moisture content, at (□) 23°C, (Δ) 70°C and (○) 100°C.

can be seen that the half-saturated specimens show an 8% decrease in fracture toughness values. This behaviour can be explained by investigating the fracture surfaces using scanning electron microscopy. At saturation, the  $G_{IC}$  values increase by about 15% compared with the dry specimen.

The toughness values for the CF/EP increase with increasing moisture through the entire range of saturation (to a maximum increase of about 64%, with a scatter of 6%). The temperature at which the specimens were soaked was found to have no influence on the fracture toughness.

Mode I tests carried out on CF/PEEK show that this material is not affected by the moisture content nor by the temperature at which the specimens were immersed. The  $G_{IC}$  value for CF/PEEK is always  $1.84 \text{ kJ m}^{-2}$ . This is in accordance with the observations of Lucas and Zhou [9].

To determine the effect of moisture on the failure mechanism, the contribution of break-energy of the different failure mechanisms were investigated, according to the proposal of Crick *et al.* [10]. The surface energy per unit area is described by the following equations, in which the critical energy release rate is divided into three contributions, one related to polymer fracture, one to peeling effects, and one to fibre fracture

$$\gamma_C = f_S \gamma_P + \gamma_R + \gamma_F \quad (4)$$

$$\gamma_P = (G_C - \gamma_R - \gamma_F) / f_S \quad (5)$$

$$\gamma_R = \gamma_P (nl\pi r + f_b) \quad (6)$$

$$\gamma_F = (\sigma_F \varepsilon_F nl\pi r^2) / 2 \quad (7)$$

where  $G_C$  is the critical energy release rate =  $\gamma_C$ ,  $\gamma_P$  is the polymer fracture energy per unit area,  $\gamma_R$  the peeling energy per unit area,  $\gamma_F$  the fibre fracture energy per unit area,  $f_S$  the surface roughness factor (dimensionless),  $f_b$  the detached fibre bundle factor

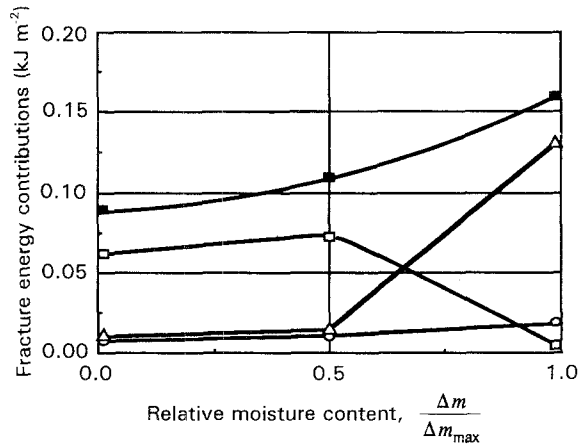


Figure 9 Fracture energy contributions for CF/EP versus moisture content. (■)  $\gamma_C$ , (□)  $\gamma_P$ , (○)  $\gamma_R$ , (△)  $\gamma_F$ .

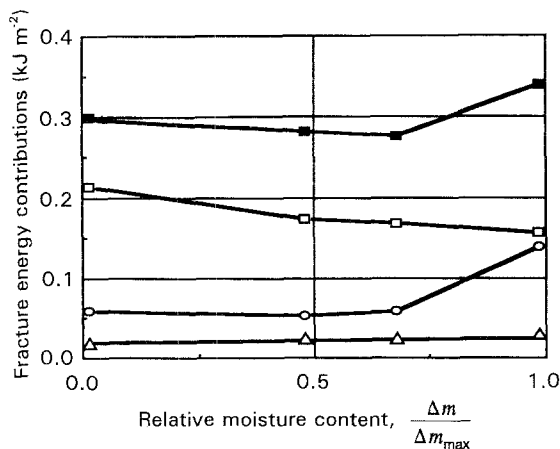


Figure 10 Fracture energy contributions for CF/EP<sub>mod</sub> versus moisture content. (■)  $\gamma_C$ , (□)  $\gamma_P$ , (○)  $\gamma_R$ , (△)  $\gamma_F$ .

(dimensionless),  $l$  the average detachment length,  $n$  the number of broken fibres per unit area,  $r$  the fibre radius,  $\sigma_F$  the fibre fracture strength, and  $\varepsilon_F$  the fibre fracture strain.

Determination of the individual contributions at different moisture contents gave the results for CF/EP and CF/EP<sub>mod</sub> shown in Figs 9 and 10. It can be seen in both diagrams that the peeling energy per unit area increases with increasing moisture content. This is verified by the observation that fibre bridging increases with moisture absorption. The contribution from the polymer energy decreases due to the bad fibre–matrix adhesion in the wet specimen, as can be noted by comparing Figs 11 and 12. From the fracture energy contribution curves, it can be seen that the greater part of the variation occurs after reaching half saturation. This fact can be explained in the following way. In the beginning the specimens were totally dry. When the samples were rested in the baths, the water entered the material at the surface. This means that at the point where the specimen is half saturated the core of the specimen is nearly dry. Because the cracks propagated in the middle of the specimens the half-saturated samples behaved more like dry specimens than wet specimens.

Scanning electron micrographs show that the dry specimens were characterized by brittle matrix fracture and good fibre–matrix adhesion. Wet specimens exhibit ductile matrix failure and poor adhesion between the fibres and the matrix.

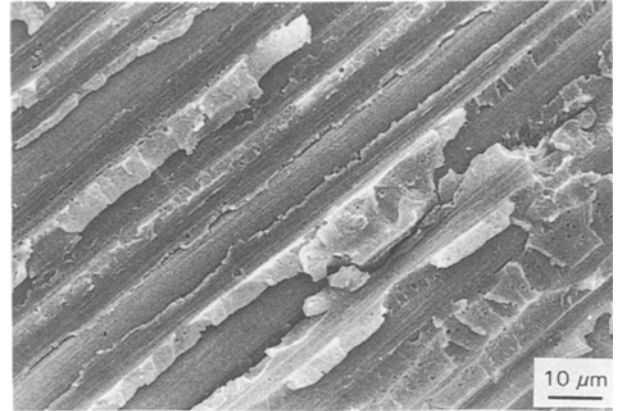


Figure 11 Fracture surface of a dry specimen in a Mode I test.

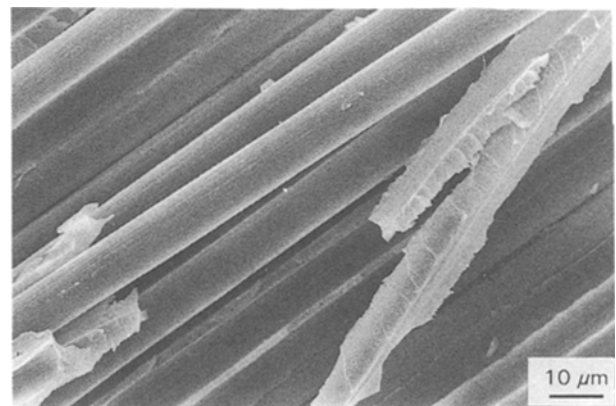


Figure 12 Fracture surface of a wet specimen in a Mode I test.

### 3.3. Mode II fracture behaviour

Mode II fracture toughness,  $G_{IIC}$ , is shown in Table I as a function of moisture content. For all three materials, it can be seen that the  $G_{IIC}$  values decrease with increasing moisture content. The decrease of the saturated specimens is, on average, about 15% compared to the values of the dry specimens for CF/EP<sub>mod</sub>, 7% for CF/EP and 20% for CF/PEEK.

The decrease of the  $G_{IIC}$  values is due to two effects. First, the fibre–matrix bonding becomes poor with increasing moisture content. The effect can be observed in scanning electron micrographs of dry and saturated specimens (Figs 13 and 14). Fracture surfaces of dry specimens show extensive hackling, whereas the saturated specimens show less hackling and many bare fibres. The large zones of bare fibres with few

TABLE I Results of the Mode II tests versus moisture content (all values in  $\text{kJ m}^{-2}$ )

Condition	$G_{IIC}$ ( $\text{kJ m}^{-2}$ )		
	CF/EP	CF/EP <sub>mod</sub>	CF/PEEK
Dry	0.41	0.64	3.90
Half saturated	0.40	0.64	3.40
Fully saturated	0.39	0.56	3.13

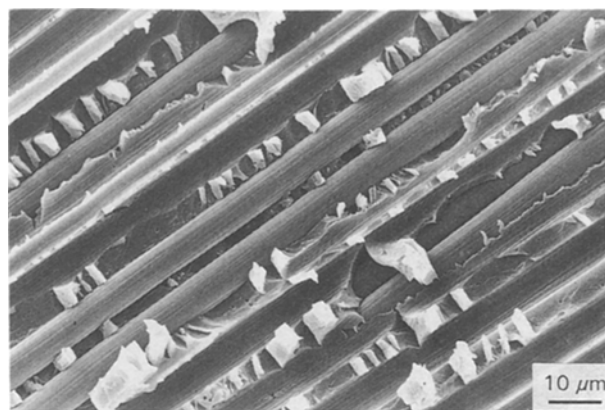


Figure 13 Fracture surface of a dry specimen in a Mode II test.

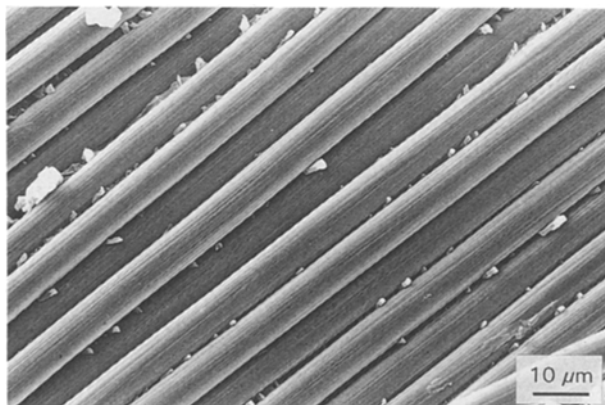


Figure 14 Fracture surface of a wet specimen in a Mode II test.

hackles point to the conclusion that the interfaces have failed and the fibres have moved without deforming the matrix. Secondly, to create hackles, less work is needed because the matrix has become soft through moisture absorption.

### 4. Conclusion

The major objective of this investigation was to evaluate the influence of moisture on crack propagation under different crack-opening modes. Three different types of materials were tested: a brittle and a modified epoxy matrix and polyetheretherketone, all reinforced with carbon fibres.

Fully saturated specimens with epoxy matrices show higher  $G_{IIC}$  values than the dry specimens. The epoxy matrix becomes soft with moisture absorption, and the fibre–matrix adhesion poorer. The  $G_{IIC}$  values of CF/PEEK are not affected by moisture, which can be explained by the low maximum moisture content of the PEEK matrix.

Comparing the results of the Mode II test for the different materials, it can be stated that all three composites show decreasing  $G_{IIC}$  values with increasing moisture content. The reduction in shear fracture toughness,  $G_{IIC}$ , was a result of the weakening of the fibre/matrix interface. Also, the increase in matrix plastification did not play an important role.

### Acknowledgements

The authors acknowledge the support of AGARD, Project G 75. Further thanks are due to BASF, Ludwigshafen, for the supply of the testing materials. Professor Friedrich is grateful for the support of the Fonds der Chemischen Industrie, Frankfurt, for his personal research activities in 1994.

### References

1. R. SELZER and K. FRIEDRICH, *Adv. Compos. Lett.* **2** (1992) 10.
2. J. VERPOEST and G. S. SPRINGER, *J. Reinf. Plast. Compos.* **7** (1988) 23
3. A. HAQUE, S. MAHMOOD, L. WALKER and S. JEELANDI, *J. Reinf. Plast. Compos.* **10** (1991) 132.
4. K. FRIEDRICH, in "Application of Fracture Mechanics to Composite Materials", edited by K. Friedrich (Elsevier Science, Amsterdam, The Netherlands, 1989) pp. 426–87.
5. C. D. SHIRRELL and J. HALPIN, ASTM STP 617 (American Society for Testing and Materials, Philadelphia, PA, 1977) pp. 514–28.
6. C. C. M. MA and S. W. YUR, *Polym. Eng. Sci.* **31** (1991) 34.
7. P. DAVIES, European Group on Fracture, Polymers and Composites Task Group, Interlaminar Fracture Testing of Composites, Ecole Polytechnique Fédérale de Lausanne, Switzerland (1990).
8. P. DAVIES *et al.*, *Compos. Sci. Technol.* **43** (1992) 129.
9. J. P. LUCAS and J. ZHOU, in "Proceedings of ICCM-9", Vol. 5, Madrid, edited by A. Miravete (Woodhead Publishing, Spain, 1993) pp. 633–41.
10. R. A. CRICK, D. C. LEACH, P. J. MEAKIN and D. R. MOORE, *J. Mater. Sci.* **22** (1987) 2094.